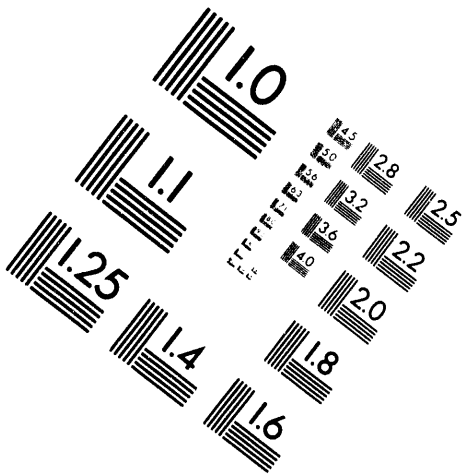




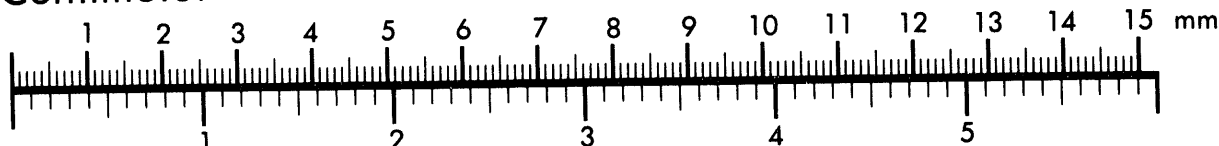
AIM

Association for Information and Image Management

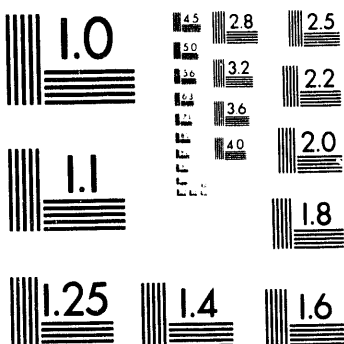
1100 Wayne Avenue, Suite 1100
Silver Spring, Maryland 20910
301/587-8202



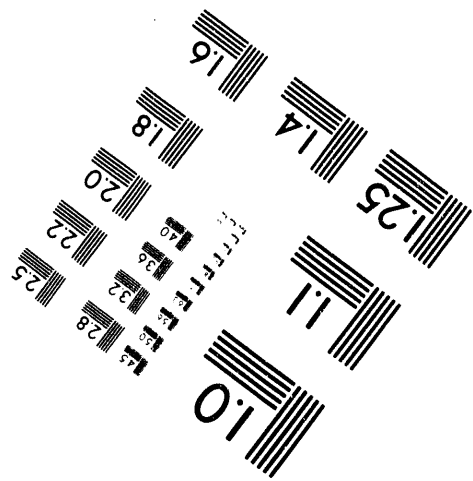
Centimeter



Inches



MANUFACTURED TO AIIM STANDARDS
BY APPLIED IMAGE, INC.



1 of 1

Conf. 9407103-24

LA-UR- 94-2809

Title:

EXPERIENCE AT THE LOS ALAMOS MESON PHYSICS
FACILITY WITH THE USE OF ALLOY INCONEL 718 AS
AN ENCLOSURE FOR A BEAM DEGRADER AND AS A
PROTON BEAM ENTRY WINDOW

Author(s):

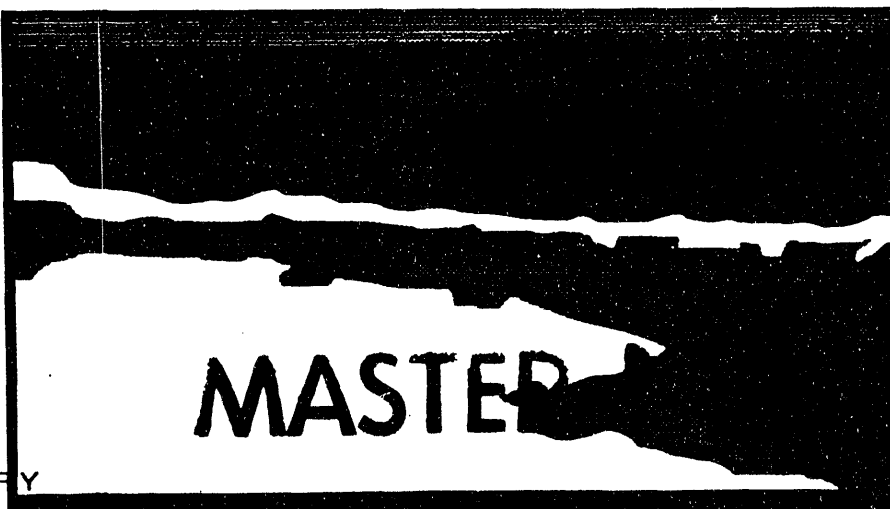
Walter F. Sommer, MTL-4
Phillip D. Ferguson, MTL-4
Robert D. Brown, AOT-4
Cecilia M. Cedillo, MTL-4
Eugene Zimmermann, NIS-6/CON

Submitted to:

US DEPARTMENT OF ENERGY

DISTRIBUTION OF THIS DOCUMENT IS UNLIMITED

Yp



Los Alamos
NATIONAL LABORATORY

Los Alamos National Laboratory, an affirmative action/equal opportunity employer, is operated by the University of California for the U.S. Department of Energy under contract W-7405-ENG-36. By acceptance of this article, the publisher recognizes that the U.S. Government retains a nonexclusive, royalty-free license to publish or reproduce the published form of this contribution, or to allow others to do so, for U.S. Government purposes. The Los Alamos National Laboratory requests that the publisher identify this article as work performed under the auspices of the U.S. Department of Energy.

Form No. 836 R5
ST 2629 1091

DISCLAIMER

This report was prepared as an account of work sponsored by an agency of the United States Government. Neither the United States Government nor any agency thereof, nor any of their employees, makes any warranty, express or implied, or assumes any legal liability or responsibility for the accuracy, completeness, or usefulness of any information, apparatus, product, or process disclosed, or represents that its use would not infringe privately owned rights. Reference herein to any specific commercial product, process, or service by trade name, trademark, manufacturer, or otherwise does not necessarily constitute or imply its endorsement, recommendation, or favoring by the United States Government or any agency thereof. The views and opinions of authors expressed herein do not necessarily state or reflect those of the United States Government or any agency thereof.

**EXPERIENCE AT THE LOS ALAMOS MESON PHYSICS FACILITY
WITH THE USE OF ALLOY INCONEL 718
AS AN ENCLOSURE FOR A BEAM DEGRADER AND
AS A PROTON BEAM ENTRY WINDOW**

Reported by

Walter F. Sommer

Phillip D. Ferguson

Robert D. Brown

Cecilia M. Cedillo

Eugene Zimmermann

BACKGROUND

Operation of the Los Alamos Meson Physics Facility (LAMPF) began in 1972 and continues at present. As is seen in Figure 1, an injector delivers protons to a 0.8 km long linear accelerator which produces a particle energy of 800 MeV; the protons are then transported to a variety of experimental areas, as seen in Figure 2. The proton beam is transported in a vacuum tube, controlled and bent by electro-magnets. The highest intensity beam, at a maximum level of 1 mA, is delivered to the experimental area designated as Area A. At the end of the experimental area, the beam is transported through an interface between beamline vacuum and one atmosphere air pressure. This interface is made of metal and is generally referred to as a beam entry window. At LAMPF, after the beam has exited the vacuum tube, it becomes incident on a number of experiments or "targets" as is seen in Figure 3. These include capsules for radiation damage studies, a beam "degrader" for the long-term neutrino experiment, and as many nine targets in the Isotope Production (IP) stringer system used to produce medically significant isotopes. Following the IP system is a beam stop used for the purpose its name implies. The beam stop also contains a beam entry window, whose purpose is to separate the 250 psig water cooling environment from 1 atmosphere of air. The beam entry window, the beam degrader, and the beam stop window are made of alloy Inconel 718, have endured a lengthy irradiation service time at LAMPF, and are the subject of this report.

Because of proton interactions with two graphite targets upstream, the proton energy has been reduced from 800 to about 760 MeV when the beam becomes incident on the vacuum-to-air beam-entry window. The particles here are essentially all protons with a small component of neutrons that backstream from the targets downstream. As the beam passes through the window, the proton irradiation experiments, the beam degrader, and the IP targets, the energy is further degraded and neutrons are created by spallation reactions. This total flux and spectrum is incident on the air to water window on the beam stop and is the radiation environment that must be used to evaluate the achieved dose on the unit. The beam degrader is exposed to a particle flux that is comprised almost entirely of protons, as shown below.

Figure 3 shows the location of the current monitor (6ACM01) used to determine the dose values given in Table 1. The profile monitor (6AHP01) is used to monitor the size, shape and position of the beam. During the period from 1985 to 1991, the beam size was maintained at a diameter of $2\sigma = 30 - 40$ mm (σ is one standard deviation in a Gaussian profile). The proton irradiation experiments place less than 20 g/cm^2 in the beam. Because of this low mass and the fact that these units were in place less than 25% of the time, their effect on the flux and spectrum at the beam stop window and beam degrader will not be considered in the following analysis. A beam degrader was in place for the entire period of time considered in this report. The configuration of the IP targets is complicated in that not all units are always in the beam and the materials in each target may be different at times. These units have a strong influence on the flux and spectrum that is incident on the beam stop window, requiring a determination of their history during the subject period; this is described below.

BEAM DEGRADER

The purpose of this unit was to provide the proper environment for Los Alamos Meson Physics Facility Experiments #E225 and #E645, both of which measured the production and character of neutrinos. Prior to 1985 when the present design was adapted, there had been difficulties with this system, not attributable to material difficulties but rather to misplacement of the unit in the proton beam in a manner that caused excessive heating. The present design [1] is shown in Figure 4. Two hemi-spherical shells (Figure 4a) made of alloy Inconel 718 are combined to make a sphere (Figure 4b). Other than a coolant

TABLE 1
OPERATING HISTORY OF THE LAMPF
WATER-TO-AIR PROTON BEAM WINDOW

LAMPF Cycle	Dates	Beam Hours	Accumulated Dose mA-hours
42	4/22-7/22/85	1252	571914
43	7/31-9/30/85	1316	713798
44	10/9-12/16/85	1440	892800
45	6/26-8/11/86	780	526481
46	8/19-10/17/86	1135	826600
47	10/24-12/15/86	1029	724564
48	6/17-7/31/87	868	636349
49	8/14-9/27/87	928	686609
50	10/16-12/01/87	894	686385
51	6/7-7/22/88	881	667446
52	8/5-10/3/88	1160	879744
53	5/4-6/18/89	925	393000
54	6/27-8/24/89	887	640000
55	8/18-9/26/89	937	675000
56	5/25-7/25/90	702	316000
57	7/10-8/26/90	963	690000
58	9/4-10/17/90	810	605000
59	6/5-7/22/94	711	327000
60	7/30-8/15/91	288	162000

water flow blockage described below, these units have operated without failure since 1985.

Assessment of the achieved fluence on the water degrader requires that the LAMPF beam history be understood. Table 1 gives this operating history for the time period of interest in this report.

A review of the experiment logs for E 225 and E645 showed that the beam degrader was in place essentially for all periods of beam operation from 1985 through July 12, 1988. The unit is interlocked to the "run permit" system of the LAMPF accelerator and automatically retracts from the beam when the coolant flow rate falls below a pre-set limit. This occurred on June 29, 1988 [2]. Review of the operations logbook [2] for this period showed that attempts to reverse the flow did not correct the difficulty. It is concluded that a blockage of the water cooling circuit had occurred resulting in several automatic withdrawals during the June 29 - July 12. The unit was removed from the beam on July 12 and replaced during the following maintenance period.

Accounting for periods when the beam degrader was out of the beam, a review of the experiments logs showed that unit was exposed to an integrated proton current of 6,490,165 μ A-hours during cycles 42-51. This level was used to determine the achieved fluence on the unit.

The geometry of the LAMPF beam stop area was simulated for calculations of proton interaction with materials and secondary particle generation and transport using the Los Alamos High Energy Transport (LAHET) Code System (LCS) consisting of LAHET coupled to the Monte Carlo Code for Neutrons and Photons (HMCNP). The vacuum-to-air beam-entry window and the beam degrader were in place for all calculations. The incident beam spot was placed at a diameter of $2\sigma = 35$ mm. The calculations determined the beam spreading due to multiple scattering, energy degradation, and secondary particle generation. In the case of the beam degrader, the calculated particle flux and spectrum was counted and averaged over a 1 cm diameter spot on the front face of the unit to account for the suspected beam drift at this location.

Combining the calculated proton flux for the modeled geometry with the measured integrated current resulted in an estimated proton fluence of 7.07×10^{21} protons/cm² and a neutron fluence of about 0.13×10^{21} neutrons/cm² with a spectrum as shown in Figure 5.

Recent calculations, also using the LCS, have estimated the radiation damage parameters for 760 MeV protons incident on alloy Inconel 718. The displacement cross section is about 3120 barn and the helium production cross section is about 210 mbarn. At the proton fluence given above, and noting that essentially all the irradiating particles are proton at about 760 MeV (Figure 5), an atom displacement level of 22.1 DPA (displacements per atom) and a helium concentration of 1485 atomic parts per million (appm) are predicted for this beam degrader.

BEAM ENTRY WINDOW DEVELOPMENT AT LAMPF

The initial beam entry window design for both the vacuum-to-air and the air-to-water interface used stepped flat plates, as shown in Figure 6. The vacuum-to-air unit was double-walled with water coolant between the stepped plates while the air-to-water interface was a single stepped plate. The material used for these "windows" was alloy Inconel 718, with a composition of 50-55%Ni, 17-21%Cr, 4-6%Nb, 3%Mo, Fe, and others. The selection criteria leading to use of alloy Inconel 718 were based primarily on excellent corrosion resistance and good weldability and compatibility with stainless steel alloys used in the cooling water manifolds.

One vacuum-to-air window failed after an estimated dose of 2.2 A-hr ($\sim 2 \times 10^{21}$ protons/cm²). Examination of the failure showed a crack in a transition area where the plate had been thinned by machining. Although not conclusive, it is expected that the crack was initiated by a scratch from the machining process. The design of the vacuum-to-air interface was changed to a doubled-walled hemi-spherical structure, reducing the stresses and eliminating the potential stress concentrations possible with the flat-plate design. During the past 10 years, these units were replaced after operating periods of 4000 hours or less, which is equivalent to an estimated proton fluence of about $3 \times 10^{21}/\text{cm}^2$ (9.3 DPA). The expected lifetime is much greater than this; the windows are changed at convenient breaks in the LAMPF operations; because the change-out is simple

and the window cost moderate, this posture does not place a time or financial burden on the accelerator while, at the same time, enhances reliability.

The flat plate design has been retained for the beam stop itself for several reasons; the geometry of this area does not allow sufficient space for the hemi-spherical design, there is no need for a double-walled configuration, the potential damage to the facility from failure is less than for the vacuum-to-air window, and the general feeling that the reason for failure observed was mitigated by careful machining and polishing techniques. The design detail has been changed from the series of steps shown in Figure 6 to a cross section that smoothly changes in cross section as a function of radius. Since it is much more difficult to replace the beam stop unit than the vacuum-to-air window, as well as much more expensive, this unit has not been replaced often. One unit was in service for seven years, from 1985-1991. The operating details are summarized in Table 1 above.

ISOTOPE PRODUCTION TARGET HISTORY AND LOADING

The configuration of the IP targets is complicated in that not all units are always in the beam and the materials in each target may be different at times. These units have a strong influence on the flux and spectrum that is incident on the beam stop window, requiring a determination of their history during the subject period; this is described below.

A survey of the LAMPF operations data for the IP targets during the 1985-1991 period showed that all of the targets were in the beam for short periods of time, all were out some of the time and, on average, 5 of the 9 IP were in the beam.

The details of the loading of the targets and the additional material in the beam from the target containers is summarized in Table 2. This is a typical loading during normal operation as reported by the IP system manager. In addition to the mass shown in Table 2, each stringer also placed 206 g of aluminum and 45 g of water in the beam.

**EFFECT OF THE ISOTOPE PRODUCTION TARGET LOADING ON
NEUTRON AND PROTON FLUX AND SPECTRUM**

As in the case for the calculations for the beam degrader, the geometry of the LAMPF beam stop area was simulated for calculations of proton interaction and secondary particle generation and transport using the Los Alamos High Energy Transport (LAHET)Code

**TABLE 2
ISOTOPE PRODUCTION TARGET LOADINGS**

Stringer	Target Material	Target Mass grams	Container Material	Container Mass grams
1	RbBr	177	Stainless Steel	276
2	ZnO	107	Al	121
3	Al	170	none	
4	Mo	470	Al	121
5	RbBr	170	Stainless Steel	276
6	KCl	98	Stainless Steel	276
7	Mo	353	Stainless Steel	276
8	Mg	210	Stainless Steel	276
9	In	448	Stainless Steel	276

System (LCS) consisting of LAHET coupled to the Monte Carlo Code for Neutrons and Photons (HMCNP). The vacuum-to-air beam entry window and the water degrader were in place for all calculations. Four configurations for the IP targets, corresponding to the

likely configurations observed during operation, were used in independent calculations. The incident beam spot was placed at a diameter of $2\sigma = 35$ mm. The calculations determined the beam spreading due to multiple scattering, energy degradation, and

TABLE 3		
NEUTRON AND PROTON FLUX AS A FUNCTION OF ISOTOPE PRODUCTION TARGET LOADING		
FOR AN INCIDENT PROTON BEAM CURRENT OF 1mA		
Case	Proton Flux $10^{13} /cm^2 s mA$	Neutron Flux $10^{13} /cm^2 s mA$
Theoretical Peak	32.7	0
<u>Tally inside a radius of 0.5 cm</u>		
All Stringers In	2.9	4.1
Stringer 9 Out	3.5	4.3
Stringer 2, 4, 6, 8 Out	5.2	5.6
All Stringers Out	17.5	14.0
<u>Tally within a radius of 3.81 cm</u>		
All Stringers In	2.0	3.6
Stringer 9 Out	2.4	3.9
Stringer 2,4,6,8 Out	3.2	4.9
All Stringers Out	8.8	10.4

secondary particle generation for each configuration. The results of these calculations for neutron and proton flux and spectrum are shown in Figures 7-10 and summarized in Table 3. The flux is averaged over two areas, a radius of 3.81 cm and a radius of 0.5 cm. Because of multiple scattering and other effects, it can be seen in Table 3 that the incident flux is relatively uniform out to a radius of 3.81 cm, varying by less than a factor of 2 from that estimated within a radius of 0.5 cm.

It would indeed be tedious to evaluate each IP stringer loading for all periods over the seven year period. The operating history was surveyed in detail and it is estimated that over the entire period, a configuration that includes Stringer 2, 4, 6, and 8 out of the beam is representative. The value for an theoretical peak is given for historical reasons. Before it was possible to model the LAMPF beam stop area in detail, we gave this value as the estimated fluence of the LAMPF air-to-water beam stop window. We did not believe that the targets would have as drastic an effect on the flux as the present calculations indicate. In fact, we believed that the fluence value originally estimated for the theoretical peak would actually be enhanced by a large number of high energy neutrons that would more than compensate for the loss in proton fluence due to scattering. As the calculations now indicate, this was an incorrect assumption.

The bounding cases are, all of the stringers in at all times and all of the stringers out all of the time. Using to 0.5 cm radius as representative of the dose rate at the center of the beam, the results showing the estimated fluence that the 1985-1991 air-to-water beam stop beam entry window endured are given in Table 4.

TABLE 4
ESTIMATED PROTON AND NEUTRON FLUENCE FOR THE LAMPF
ALLOY INCONEL 718 BEAM ENTRY WINDOW
Tally Radius = 0.5 cm

Case	Fluence - $10^{21} / \text{cm}^2$		
	Proton	Neutron	Proton plus Neutron
All Stringers In	1.21	1.71	2.92
Stringers 2, 4, 6, 8 Out	2.17	2.33	4.50
All Stringers Out	7.30	5.84	13.14
Theoretical Peak	13.65	0	13.65

The proton fluence for the case when stringers 2, 4, 6, and 8 are out of the beam results in a displacement level of 6.7 DPA and a helium concentration of 456 appm. In addition, the neutron flux associated with this configuration adds an estimated displacement level of 0.95 DPA (by applying the fluence to displacement ratio as given in Reference 6 for the Engineering Breeder Reactor II, EBR-II).

EXPERIENCE WITH THE IRRADIATION PERFORMANCE OF ALLOY INCONEL 718 AS FOUND IN THE LITERATURE

Alloy Inconel 718 has been considered a candidate for the first wall of a fusion reactor. There is a limited amount of data on the irradiation performance of this material in a fission reactor environment; this data is summarized below. All neutron fluences quoted below are for $E > 0.1$ MeV.

Swelling

Powell et al. [4] found less than 1% swelling for heat treated material irradiated to a fluence of 1.8×10^{23} n/cm² (85 DPA) at 400 - 650 °C in EBR-II. Garner and Gelles measured less than 1% swelling in this alloy, also heat treated, after a fluence of 2.8×10^{23} n/cm² (140 DPA) at 400 °C in EBR-II. These data indicate that swelling is controlled for alloy Inconel 718 irradiated in a fission reactor especially where helium production by transmutation is relatively low.

Fracture Toughness

Michel and Gray [6] measured fracture toughness by the J-Integral method and found a decrease from 120 to 65 kJ/m² after a fluence of 2.2×10^{22} n/cm² (12DPA) for heat treated and aged material irradiated in EBR-II at a temperature of 427 °C. They also observed that the flow stress increased from 150,000 to 160,000 psi from this irradiation.

Fatigue Crack Growth Rate

Early studies by Mitchel and Smith [7] found no effect of irradiation at a fluence of 5×10^{22} n/cm² (25.5 DPA) at EBR II at 427 °C. The authors cautioned that the inclusion of helium at temperatures above 500 °C may affect the crack growth rate. In later work [8], they found that the crack growth rate was sensitive to hold time between tensile load

application. The tests were conducted at a frequency of 0.17 Hz. After a fluence of 1.4×10^{22} n/cm² in EBR-II at 427 °C, no effect on fatigue crack growth rate was found for continuous cyclic loading. The crack growth rate increased by 10 times when a 1 minute hold time was used. The result was attributed to a helium diffusion effect at the crack tip. In still later work [9], they found that both continuous and a 1 minute hold time increased the crack growth rate by up to 10X in the loading range of 10 to 60 MPa m^{1/2}. These tests were on heat treated material irradiated at EBR-II at 650 °C to a dose of 16-18 DPA. They later refined their analysis [10] and reported that the increase of crack growth rate for irradiated as opposed to unirradiated material was 2 times for the "no hold-time" case and 10 times for the 1 minute hold-time case.

Another researcher, James [11], found no increase in fatigue crack growth rate for heat treated plate material irradiated at EBR-II to 28 DPA at 427 °C. There was a small effect noted on one type weldment studied.

Radiation Hardening

Ward et al. irradiated the subject alloy in EBR-II to a fluence of 6.6×10^{22} n/cm² at 400 - 650 °C. Classical radiation hardening was observed. Tests performed at temperature greater than 538 °C showed a loss in ductility and was explained as an effect of helium in the material.

Brown and Cost irradiated annealed and heat treated samples in an 800 Mev proton beam to a fluence of 2.2×10^{19} protons/cm² in a direct water cooled enclosure at a temperature of about 40 °C. The annealed material hardened slightly and suffered a small loss in ductility while the heat treated material softened slightly with no apparent effect on ductility.

Microstructure

Bell and Lauritzen [14] studied the microstructural changes caused by exposure to the neutron flux at EBR-II to a fluence of 6×10^{22} n/cm² at 626 - 725 °C. They observed a slight aging and the formation of η phase platelets, but did not conduct any mechanical property measurements.

CONCLUSIONS AND RECOMMENDATIONS

1. A beam degrader made of alloy Inconel 718 and used at LAMPF endured an estimated displacement damage level of 22.1 DPA and a transmutation-induced helium concentration of 1485 appm. The water-to-air beam entry window used on a beam stop at LAMPF was irradiated to an estimated damage level of 6.7 DPA from protons and 0.95 DPA from neutrons; the helium concentration is estimated at about 456 appm.

Reference 15 indicates that the He-3 Accelerator Production of Tritium (APT) design will expose the beam entry window to a damage level of about 25 DPA per operation-year. Our phenomenological experience in a prototypic environment for APT at LAMPF then implies at least a one year life time for this material. It is generally held that this alloy can perform for substantially longer times than the present data indicates. Dedicated experiments and property measurements are needed to determine the extended life time of this material.

2. From a limited data base from irradiation with fission reactor neutrons, it appears that the microstructure is stable.
3. Data from fission reactor irradiations indicate that swelling is very low at very high doses for moderate levels of helium concentration.
4. Fracture toughness decreases by a factor of two after fission reactor irradiation to 12 DPA; this initially tough material is still quite tough at this damage level.
5. Fatigue crack growth rate, measured in pre-cracked compact tension specimens, is increased after irradiation to 15 -20 DPA in a fission reactor environment. The effect of a hold time is seen to increase the rate by 5 - 10 times, generally attributed to an effect from helium concentration.

The phenomenological data from the LAMPF components described above are from materials that were subjected to a very large number of thermal stress-induced loading and

unloading sequences per day as the accelerator trips off and is turned back on. This is a comparable effect to the tests described in terms of hold time. Also, the helium concentration to displacement level ratio from exposure to 760 MeV protons, relative to a fission reactor neutron environment, is 100 times or so greater. Thus 760 MeV proton irradiated material endured a relatively high damage level under conditions of a cyclic stress and high helium concentration.

6. A systematic study of mechanical property and microstructural changes caused by proton irradiation of alloy Inconel 718 to high dose would aid the understanding of the response of this alloy and also aid in life time predictions.

REFERENCES

1. Los Alamos National Laboratory Drawing 70Y-158868, J. E. Vasquez, November 1984.
2. Los Alamos National Laboratory Notebook R 6852, pp 27-31, T. Newland, June,-July 1988.
3. Monroe S. Wechsler et al., "Spallation Radiation Damage and Dosimetry for Accelerator Transmutation of Waste Applications," Los Alamos National Laboratory Report LA-UR-93-3435,(Sept 1993), to be published in ASTM STP 1228.
4. R. W. Powell, et al., "Swelling of Several Commercial Alloys Following High Fluence Neutron Irradiation", J. Nucl. Mater 103&104(1981)969-974.
5. Frank A. Garner and David S. Gelles, "Neutron-Induced Swelling of Commercial Alloys at Very High Exposures," ASTM STP 1046 (1990), pp. 673-683.
6. D. J. Michel and R. A. Gray, "Effects of Irradiation on the Fracture Toughness of EBR Structural Materials," J. Nucl. Mater. 148 (1987) 194-203.
7. D. J. Michel and H. H. Smith, "J. Nucl. Mater. 85&86 (1979) 845-849.

8. D. J. Michel and H. H. Smith, "Effect of Neutron Irradiation on Fatigue and Creep-Fatigue Crack Propagation in Alloy 718 at 427 °C," *J. Nucl. Mater.* 122&123 (1984) 153-158.
9. H. H. Smith and D. J. Michel, "Effect of Neutron Irradiation on Fatigue Crack Propagation in Alloy 718 at 650 °C," *Letter to the Editor*, *J. Nucl. Mater.* 137(1985) 81-85.
10. H. H. Smith and D. J. Michel, "Neutron Irradiation Effects on Fatigue Crack Propagation in Alloy 718 at 650 °C," *Letter to the Editor*, *J. Nucl. Mater.* 149 (1987) 109-112.
11. Lee A. James, "The Effect of Fast Neutron Irradiation Upon the Fatigue-Crack Propagation Behavior of Alloy 718 Plate and Weldments," *J. Nucl. Mater.* 136 (1985) 91-96.
12. A. L. Ward, J. M. Steichen, and R. L. Knecht, "Irradiation and Thermal Effects on the Tensile Properties of Inconel 718," *ASTM STP 611* (1976) pp 156-170.
13. R. D. Brown and J. R. Cost, "Mechanical Properties of 800-MeV Proton Irradiated Metals," *ASTM STP 782* (1982) pp 917-926.
14. W. L. Bell and T. Lauritzen, "Microstructural Changes in Neutron-Irradiated Commercial Alloys: A Sequel," *ASTM STP 782* (1982) pp. 139-151.
15. APT ^3He Target/Blanket Topical Report, Los Alamos National Laboratory Report LA-CP-94-27. Volume 1, Revision 1, March 1994.

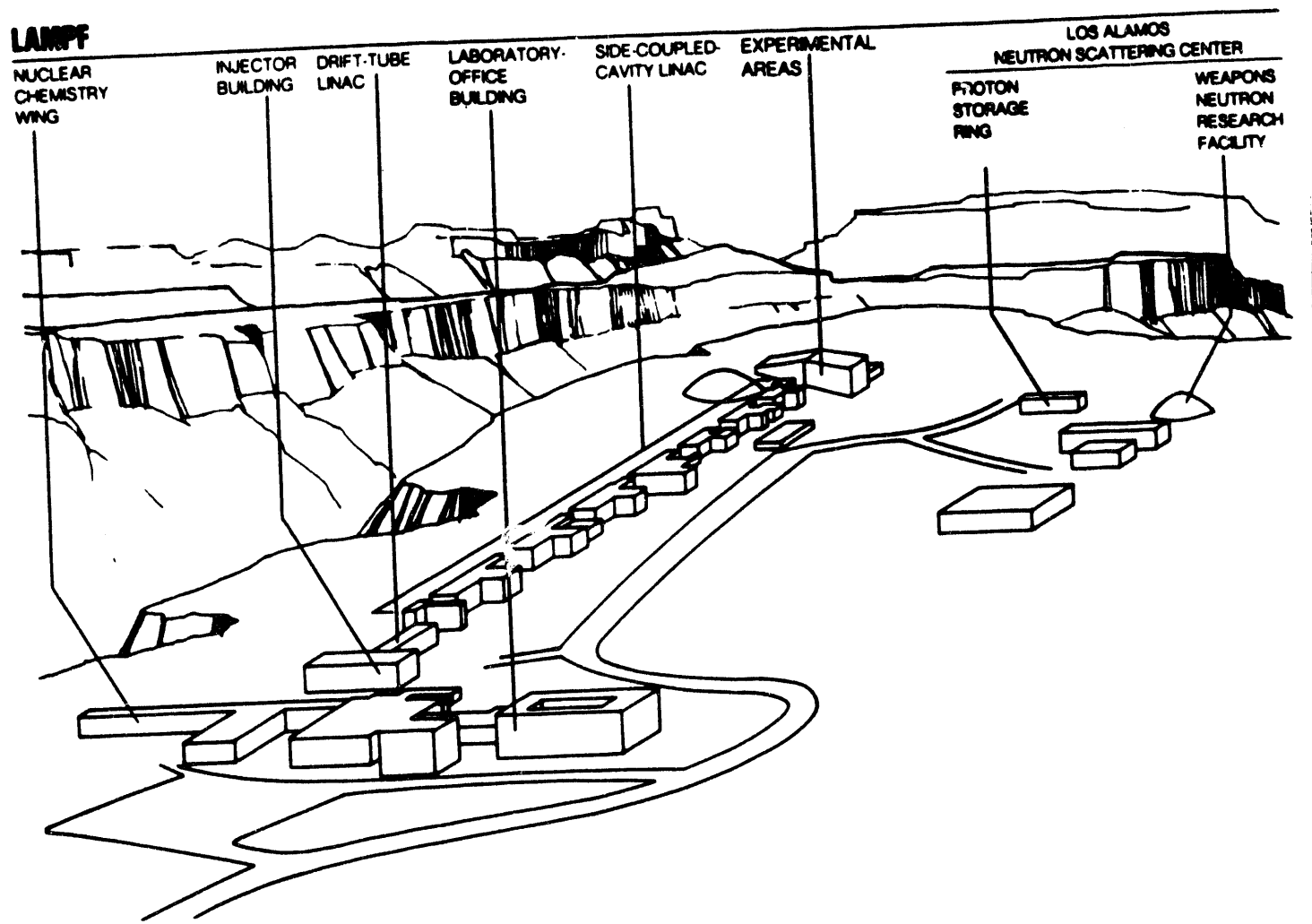


FIGURE 1. Layout of the Los Alamos Meson Physics Facility showing the injector, the linear accelerator, and the experimental areas.

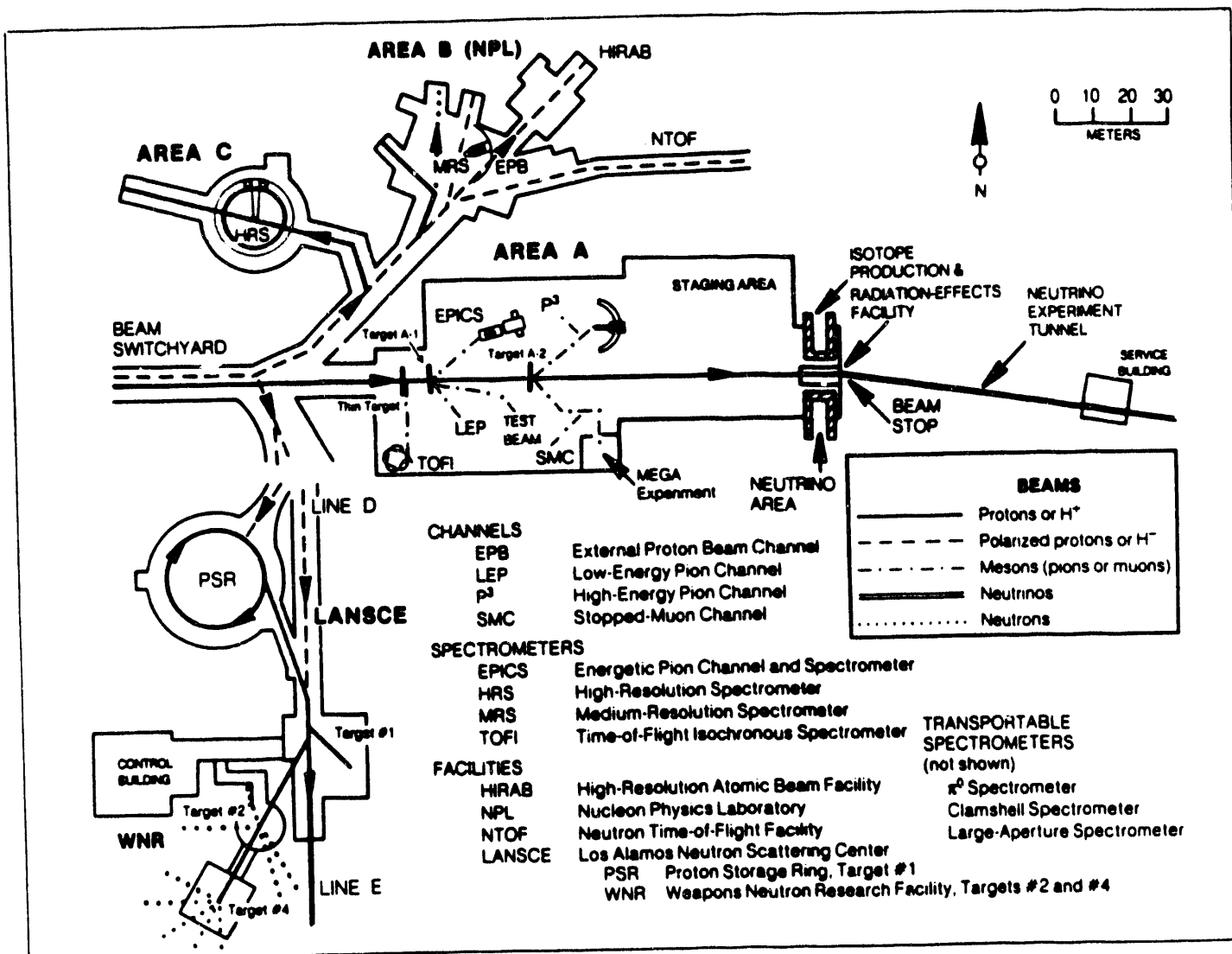


FIGURE 2. The layout of the LAMPF experimental areas showing the location of the beam stop where the beam degrader, the vacuum-to-air and the water-to-air windows made of alloy Inconel 718 are used.

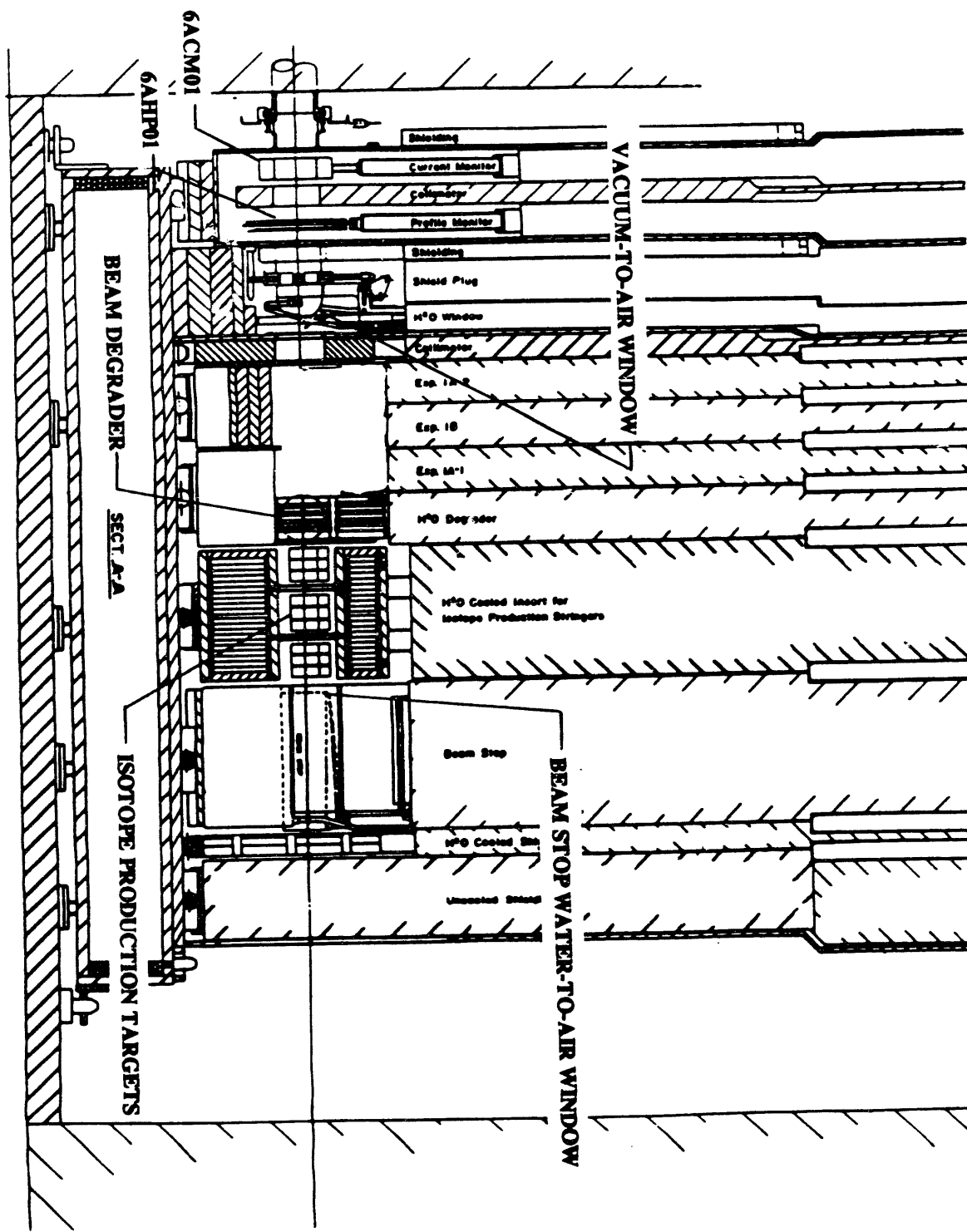


FIGURE 3. Layout of the LAMPF beam stop area showing the location of the vacuum-to-air window (H_2O Window), the beam degrader (H_2O Degader), the Isotope Production area, and the beam stop.

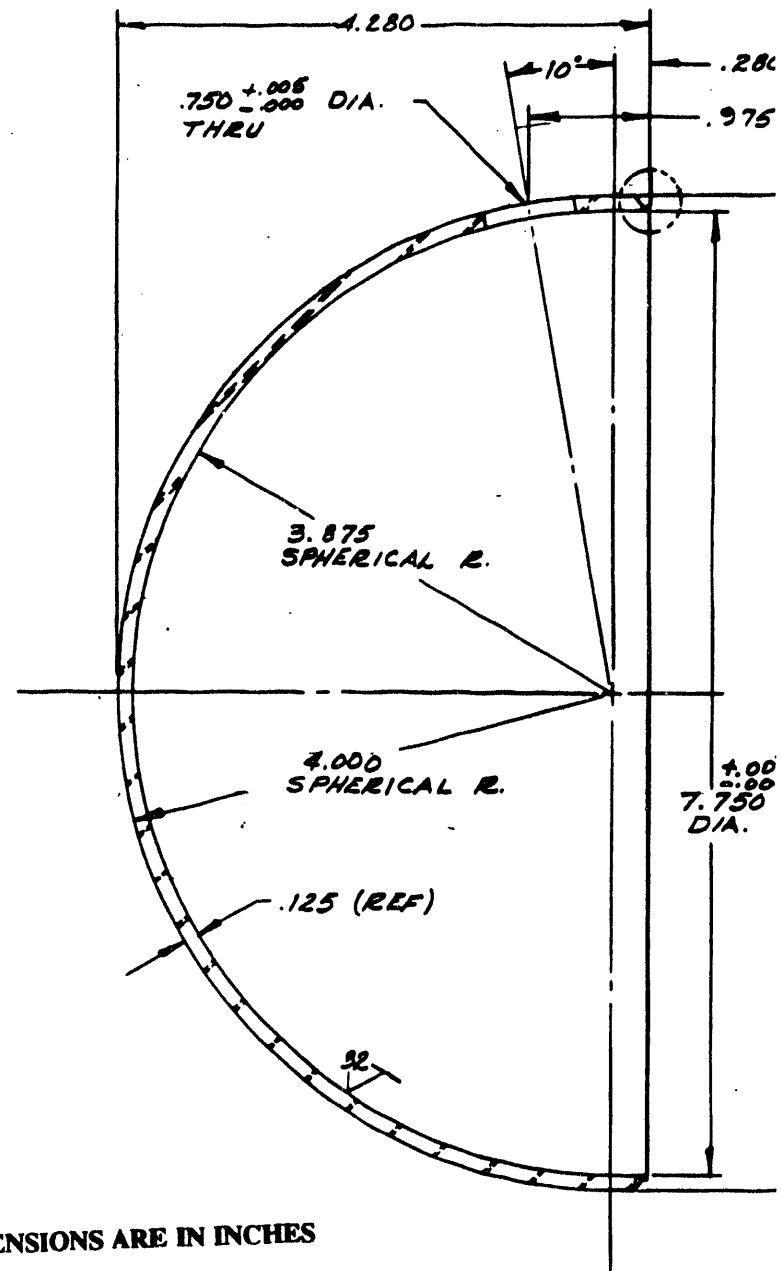


FIGURE 4a. Detail of the hemispherical shell made of alloy Inconel 718 used to construct the beam degrader.

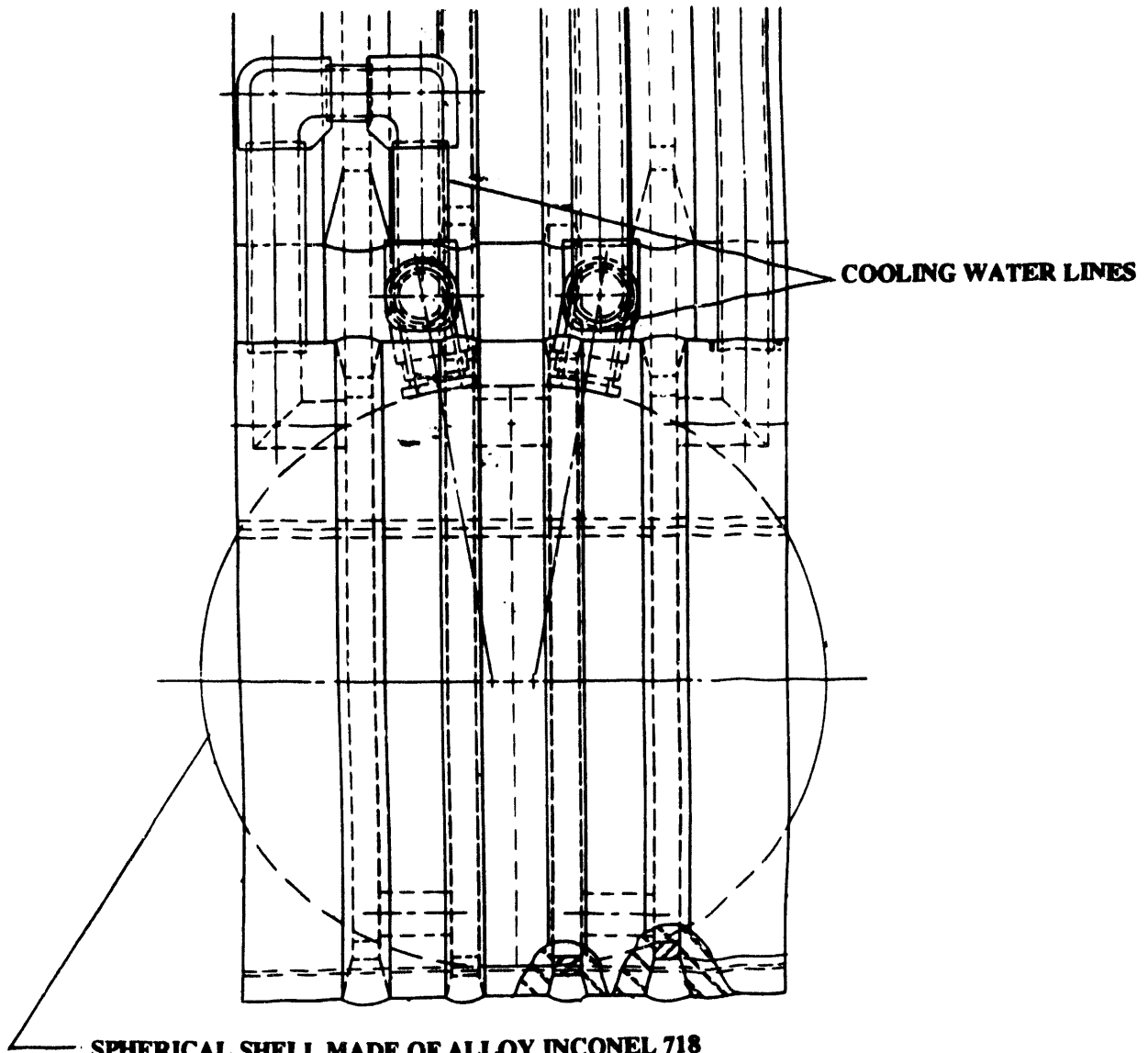


FIGURE 4b. Assembly of the beam degrader.

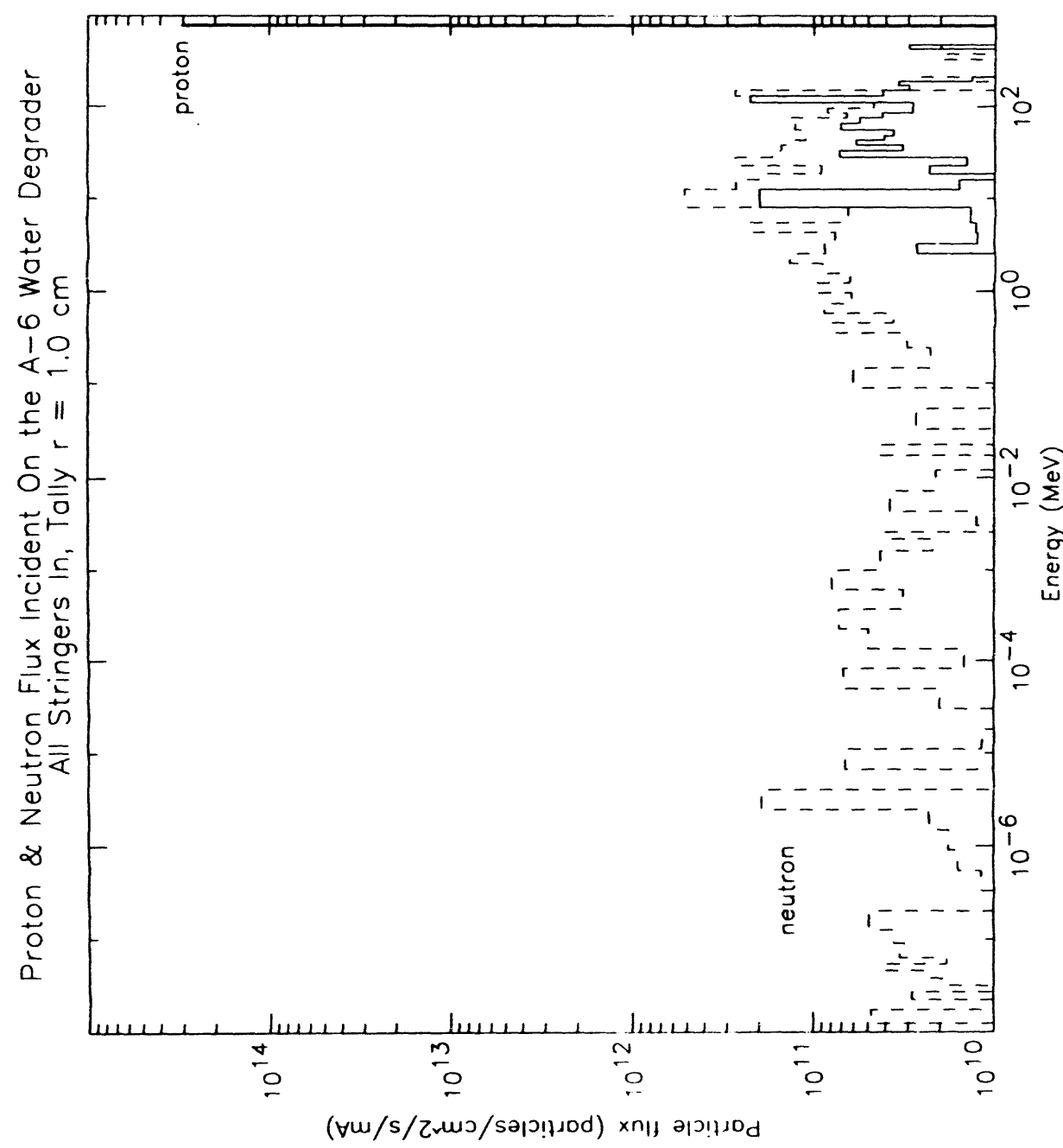


FIGURE 5. Calculated particle flux spectrum on the beam degrader.

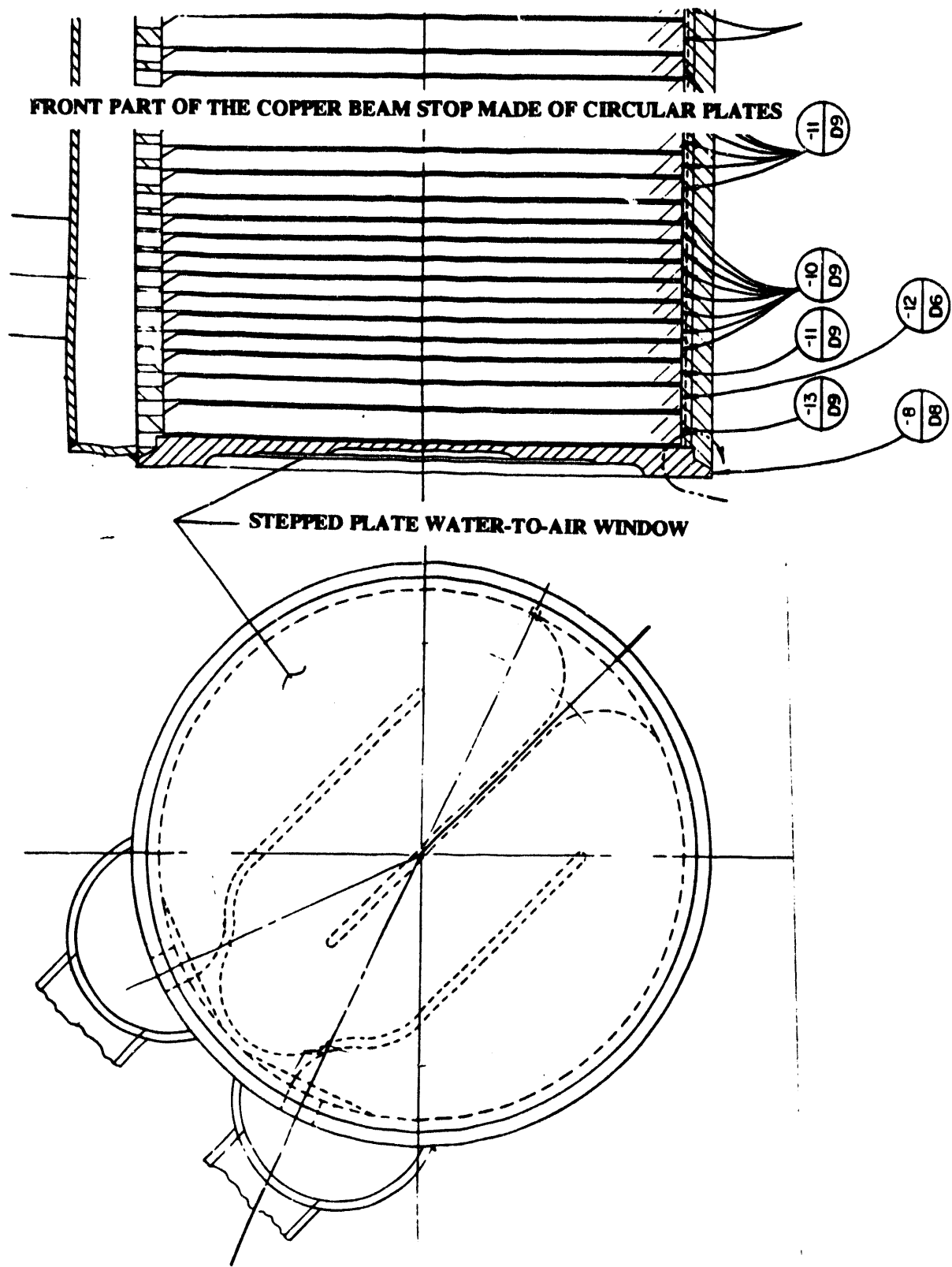


FIGURE 6. Description of the stepped "flat plate" window used on the beam stop.

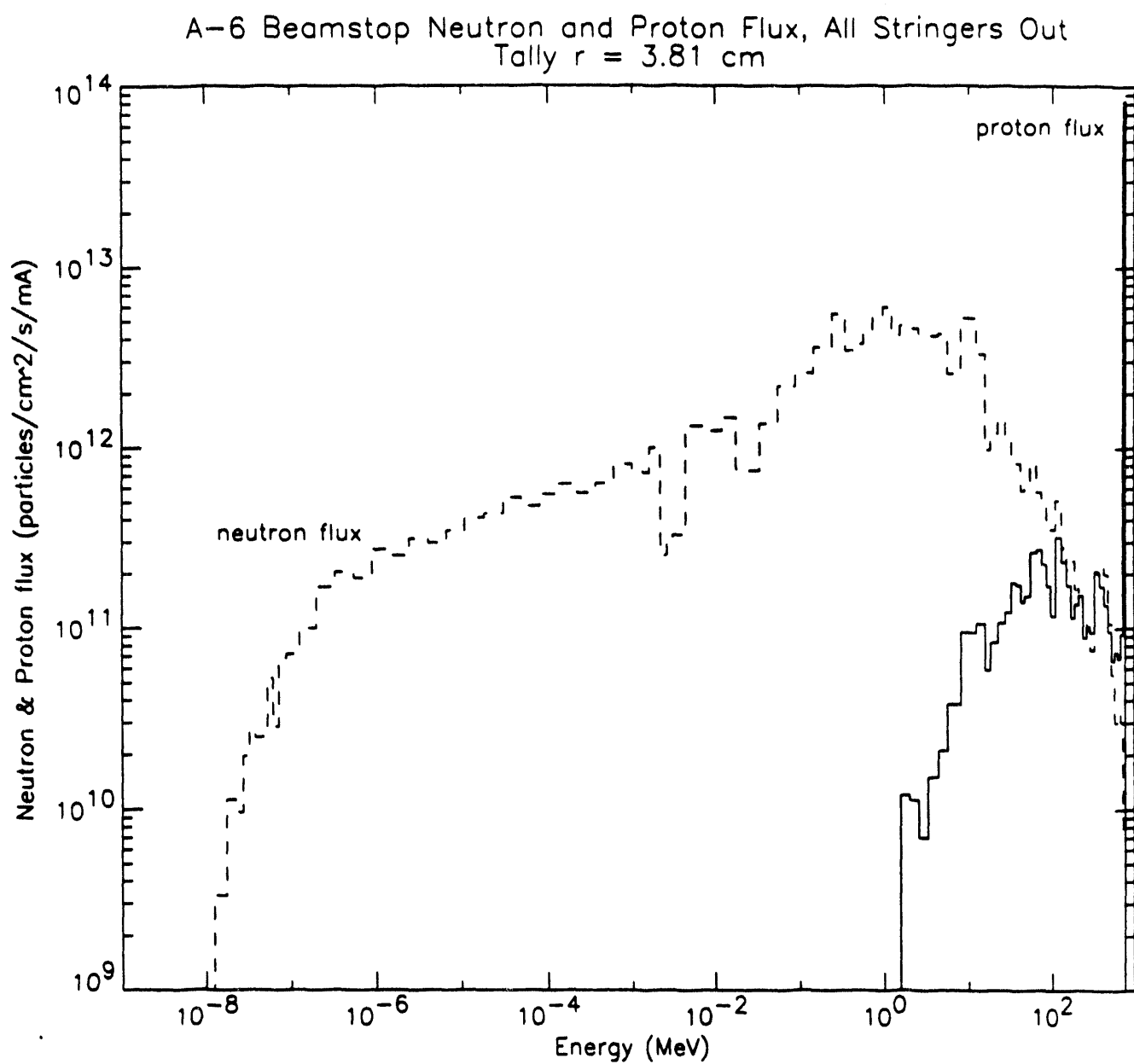


FIGURE 7. Neutron and proton flux and spectrum calculated for a simulated Target A-6 (beam stop) geometry - All Isotope Production targets are out of the beam.

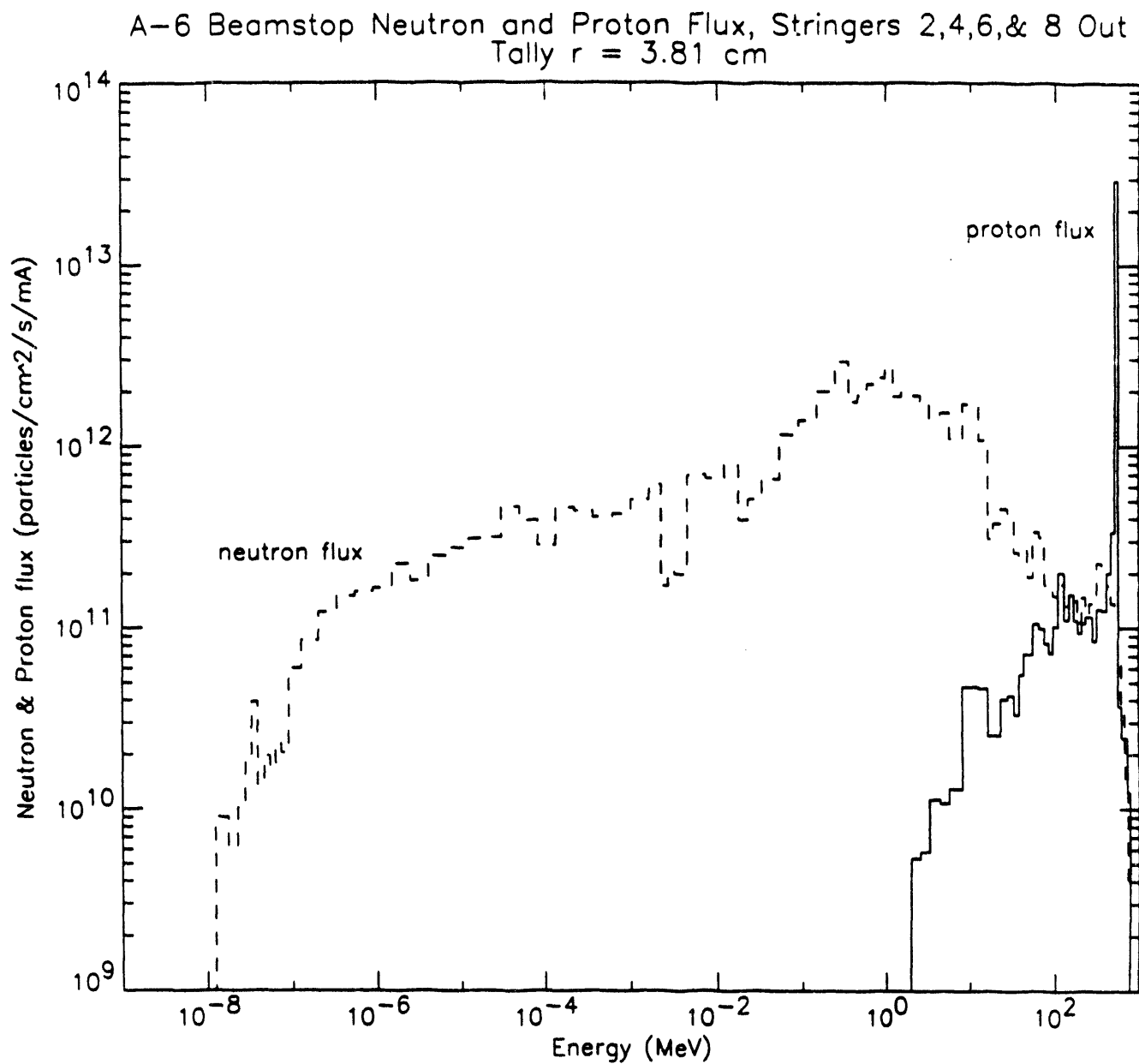


FIGURE 8 Neutron and proton flux and spectrum calculated for a simulated Target A-6 (beam stop) geometry - Isotope Production targets 2, 4, 6, and 8 are out of the beam.

A-6 Beamstop Neutron and Proton Flux, Stringer 9 Out
Tally $r = 3.81$ cm

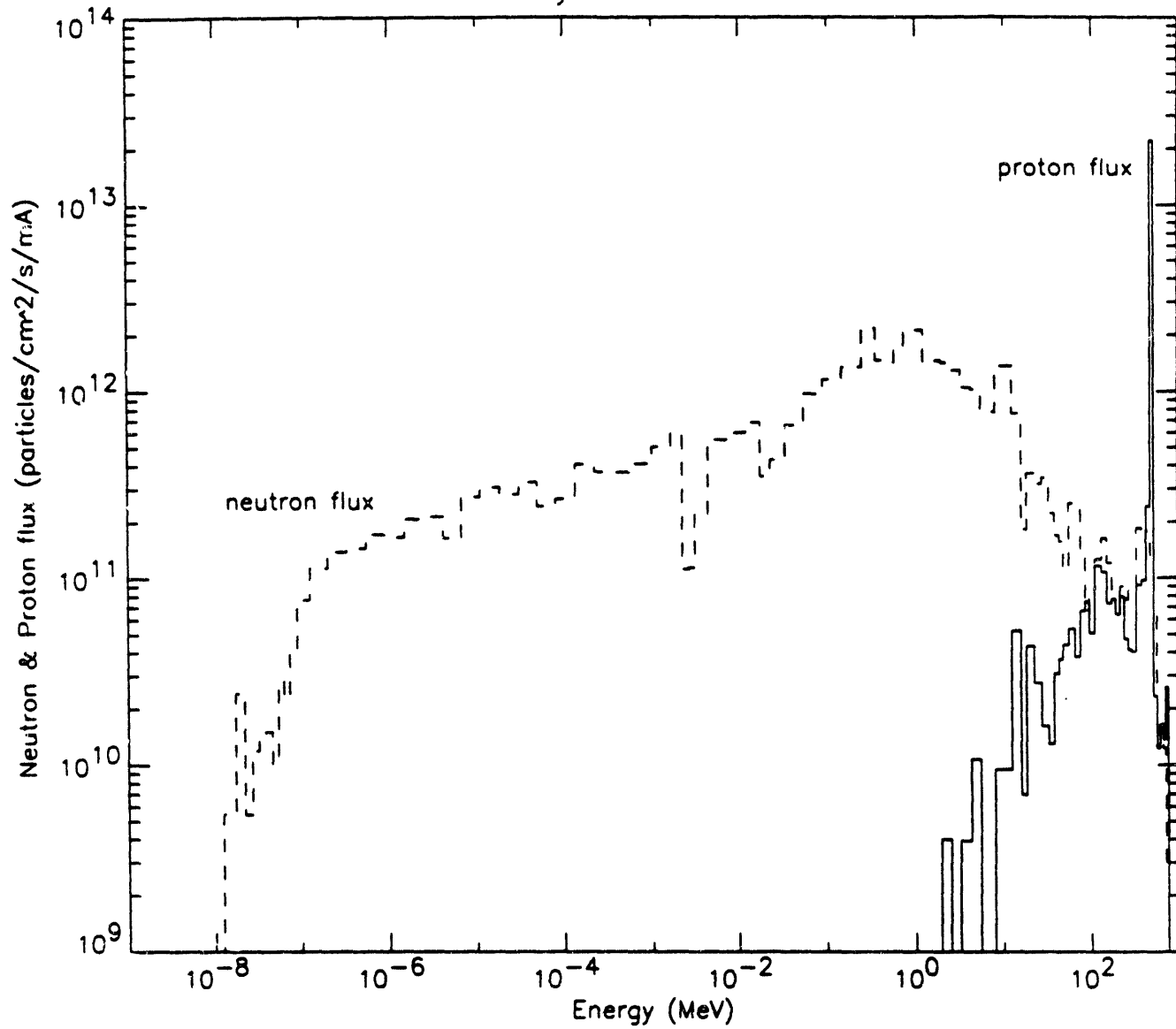


FIGURE 9. Neutron and proton flux and spectrum calculated for a simulated Target A-6 (beam stop) geometry - Isotope Production target 9 is out of the beam.

A-6 Beamstop Neutron and Proton Flux, All Stringers In
Tally $r = 3.81$ cm

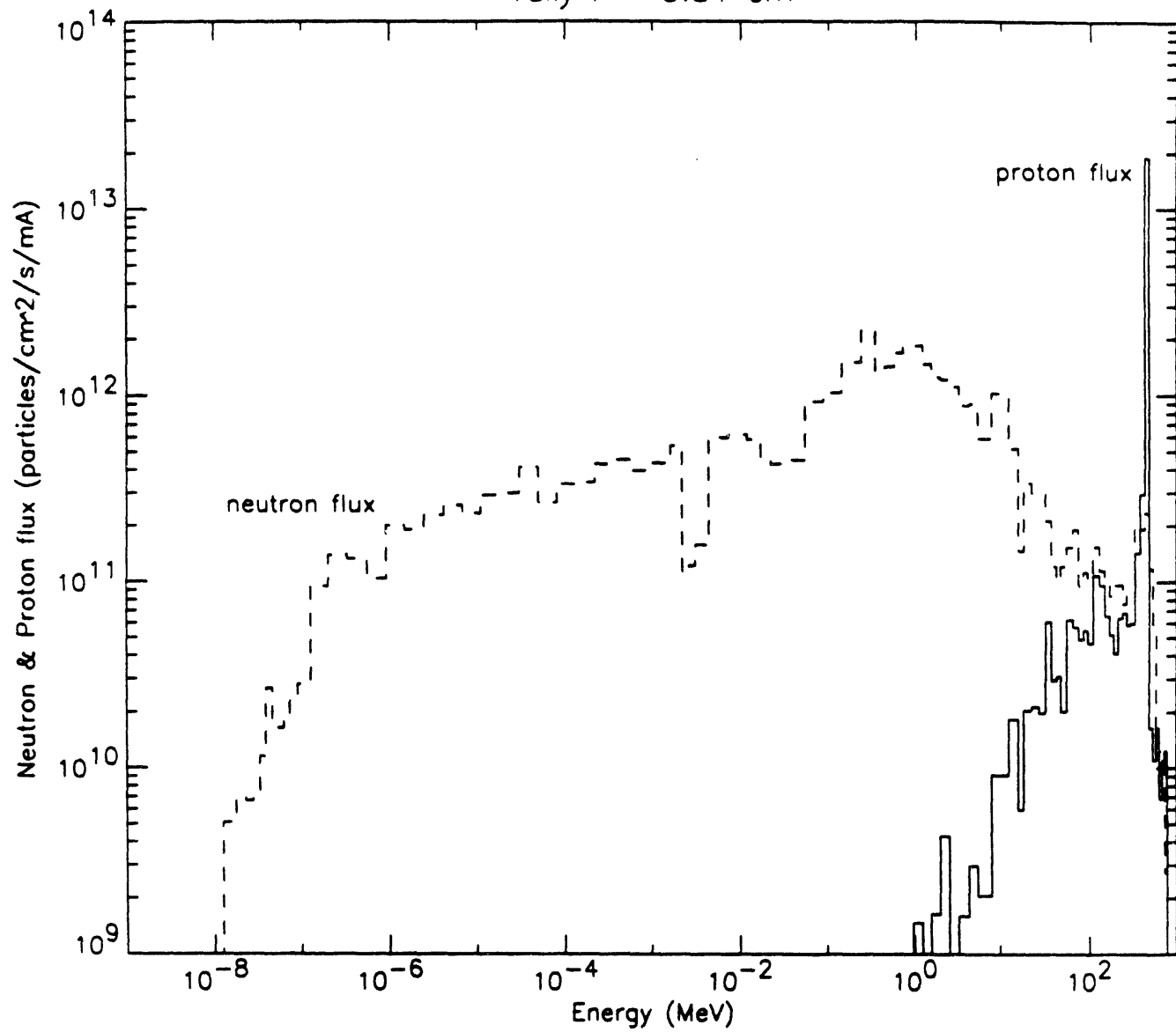


FIGURE 10. Neutron and proton flux and spectrum calculated for a simulated Target A-6 (beam stop) geometry - All Isotope Production targets are in the beam.

**DATE
FILMED**

10/18/94

END

